



Demystifying DGE-AUC Part 1: Back to the Basics

Akash Bhattacharya
Beckman Coulter Life Sciences, 4510 Byrd Dr, Loveland, CO 80538

Abstract

This application note is the first in a technical series which will cover the basics of density gradient equilibrium analytical ultracentrifugation or DGE-AUC. In this first installment, we introduce the basics of AUC followed by a comparison of the different AUC techniques and their use cases. Then we discuss the theoretical background of density gradients, and the basics of DGE-AUC, a method which is orthogonal to sedimentation velocity or SV-AUC as well as sedimentation equilibrium or SE-AUC. We conclude covering how DGE-AUC gradients can be simulated and the utility of these simulations.

Introduction

Background

Analytical ultracentrifugation (AUC) is a versatile technique for quantification of the biophysical properties of analytes in solution. AUC was invented nearly a century ago by Theodor Svedberg, whose pioneering work in determination of molecular weights of proteins and colloids was awarded the Nobel Prize in Chemistry in 1926. Not coincidentally, this was also the year that Jean Perrin was awarded the Nobel Prize in physics for his work on the sedimentation equilibria of particles in suspension, which provides much of the theoretical underpinning to experimental AUC¹⁻³. Advancements in instrumentation allowed the AUC to find utility in a wide range of biophysical systems⁴. In 1958, AUC played a crucial role in one of the most significant biophysical discoveries to date. Meselson and Stahl employed AUC to characterize the DNA extracted from *E. coli* grown in heavy isotope (¹⁵N or ¹⁵N/¹⁴N) mixed media by centrifuging the nuclear extract in a cesium chloride (CsCl) gradient. Since ¹⁵N labeled DNA is denser than ¹⁴N labeled DNA, the equilibrium radial position of the DNA during CsCl centrifugation corresponds to the heavy/light isotope fraction of the DNA. This experiment confirmed the Watson/Crick semiconservative model of DNA replication⁵. Today we refer to this technique as Density Gradient Equilibrium Analytical Ultracentrifugation (DGE-AUC). This application note will discuss the theory and application of DGE-AUC in the modern Optima AUC instrument.

AUC 101

The physical processes occurring inside an analytical ultracentrifuge during an experiment can be understood as follows: Under conditions of constant rotor speed, an analyte particle experiences two opposing forces. Centrifugal acceleration drives the particles toward the bottom of the sample tube, while diffusion tends to distribute the particles uniformly throughout the tube. With the use of an optical detection system, it is possible to measure the velocity of analyte particles through the tube over the course of the experiment. In addition, the centrifugal acceleration is known, as it is an experimental parameter. The ratio of these two quantities (analyte velocity (v) divided by centrifugal acceleration ($\omega^2 r$)) is known as the sedimentation coefficient (S) of the analyte particle. The International System of Units (SI) for sedimentation coefficient is seconds, while the practically used unit is 10^{-13} seconds, which is known as one Svedberg. The sedimentation coefficient of an analyte particle (S) is directly proportional to its buoyant mass (M_b) and inversely proportional to its Stokes frictional coefficient (f) and is therefore inversely proportional to its radius and shape (anisotropy).

$$S \equiv \frac{v}{\omega^2 r} = \frac{M_b}{f}$$

This relationship is known as the Svedberg equation and allows for a direct interpretation of the sedimentation coefficient, which is an experimentally determined quantity, to the mass, size and shape of the analyte particle, which are of course the fundamental biophysical properties of the analyte that we are ultimately interested in finding⁶⁻⁸.

The Stokes frictional coefficient (f) for a non-spherical analyte is shown below. In this equation, η is the liquid viscosity, v is the sphere's velocity through the liquid, R_s is the Stokes' radius (which is the radius of a sphere with the same frictional coefficient as the non-spherical analyte particle (f), but crucially - not the same mass and density).

$$f = 6\pi\eta R_s v$$

The Stokes frictional coefficient (f_o) for a perfect sphere of the same mass and density of the non-spherical analyte particle is:

$$f_o = 6\pi\eta R_o v$$

where, R_o is the radius of the sphere. The ratio f/f_o is a measure of the anisotropy of the non-spherical analyte particle. The frictional coefficient can be related to the diffusion coefficient via the Stokes-Einstein relation:

$$D = \frac{k_B T}{f}$$

Here, k_B is the Boltzmann constant, and T is the temperature.

In simple terms, an SV-AUC experiment measures particle velocity (v) as a function of radius (r) and time (t) as the analyte particles sediments (or floats). Using this measured parameter, and by including the known value of rotational acceleration ($\omega^2 r$), it is possible to determine the sedimentation coefficient (or S -value) of analyte particles from first principles. However, this analysis (based on the Svedberg equation, and discussed in more detail in the section on Analytical Band Centrifugation later) does not separately provide the diffusion coefficient and mass of analyte particles. These can be obtained via a more sophisticated approach pioneered by Ole Lamm in the 1930s⁸, which is widely used today and lends itself to high-resolution characterization of sample heterogeneity.

Comparison of AUC Methods

Sedimentation-Velocity AUC

Returning to the events occurring during the AUC experiment, if the centrifugal acceleration dominates over diffusion (i.e., the particle flux toward the cell bottom due to sedimentation is greater than the back-diffusion flux due to Brownian motion), then as the experiment progresses the analyte particles will be observed to travel to the bottom of the sample cell and accumulate in the form of a pellet at the end of the experiment. As the experiment progresses, there will be a depletion of analyte particles from the top of the cell. A transition layer will be observed between the zone of depletion and the rest of the cell where particles exist at a constant concentration. This transition zone is known as the boundary, and as the experiment progresses the boundary moves from the meniscus, which is at the top of the cell, all the way to the bottom of the cell as the pellet accumulates. The shape of this boundary depends upon the diffusion properties of the analyte particle. This type of experiment is known as a sedimentation velocity (SV-AUC) experiment and is one of the most-used AUC experiments today. The twin phenomena of sedimentation and diffusion are described by the Lamm partial differential equation, which takes into account the sector shape geometry of an AUC cell^{8,9}.

$$\frac{\partial c}{\partial t} = D \left(\frac{\partial^2 c}{\partial r^2} + \frac{1}{r} \frac{\partial c}{\partial r} \right) - S\omega^2 \cdot \left(r \frac{\partial c}{\partial r} + 2c \right)$$

In this equation, analyte concentration c is a function of both radius (r) and time (t). The diffusion coefficient is represented by D and the sedimentation coefficient by S . The angular velocity is ω . There have been several approximate solutions of the Lamm equation⁸⁻¹⁴ over the years. However, the use of finite element methods and their implementation in modern computers has allowed for accurate numerical solutions of the Lamm equation using the large datasets obtained from a modern AUC instrument¹⁴⁻¹⁷. SV-AUC experiments are carried out in AUC cells, typically with 2-sector centerpieces¹⁸. Each sector is loaded with ~ 400 μ L of solution, which leaves a small “air gap” region at the top (radially inward) of each sector. The reference sector is loaded with buffer, while the sample sector is loaded with the target analyte solution. The AUC absorbance detector system records light intensity as a function of radius for both sectors ($I_{reference}$ and I_{sample}), and converts the intensity readings into absorbance readings using the formula:

$$Abs = -\log \frac{I_{reference}}{I_{sample}}$$

This calculation eliminates the contribution of buffer light absorption. It is possible to conduct this experiment with target analytes loaded into both sectors, effectively doubling experimental throughput. In this case, the absorbance is calculated using the formula:

$$Abs = -\log \frac{I_{air-gap}}{I_{sample}}$$

where $I_{air-gap}$ is the light intensity obtained from the air-gap region at the top of the cell. However, since the value of $I_{air-gap}$ is a single point value and not measured for all radii, care must be taken to perform radial baselining of the data. This is usually done via some form of time invariant noise correction in the various software packages, most notably UltraScan and Sedfit^{14-17,19-22 23-26}.

SV-AUC in gene therapy

Sedimentation-velocity experiments have become recognized as the gold standard²⁷ in the characterization and quantification of adeno-associated virus (AAV) population distributions. AAV is a widely used vector that has shown tremendous potential for gene therapy. Production of AAV capsids from mammalian cell lines usually results in a population that contains fully loaded capsids, which contained the complete therapeutic ssDNA gene of interest (GoI), empty capsids, which do not contain any DNA cargo at all, and a range of partially loaded capsids, which contain some but not the complete GoI²⁸⁻³⁰. Thus, characterizing the population distribution of AAV capsids and, specifically, determining the loading fraction (defined as % of fully loaded AAV capsids), is an important step in drug quality control³¹⁻³⁴. SV-AUC experiments are highly useful in this context because they provide excellent resolution of empty, fully loaded and partially loaded AAV capsids down to baseline resolution³³. In addition, SV-AUC experiments also provide quantitation of aggregates and fragments of gene therapy vectors.

Analytical-Band AUC

Also known as Band-Sedimentation (BS) AUC, this is a variant of the SV-AUC experiment, where a very small volume (~ 15 µL) of the target analyte is loaded into a small reservoir at the top of a special two-sector cell with a “band-forming” centerpiece¹⁸. This reservoir is connected to the sector via a capillary. The sector itself is loaded with the usual ~ 400 µL of buffer. When centrifugation begins, analyte is forced by pressure through the capillary and layered on top of the buffer in the sector. Thereafter, the analyte proceeds to sediment to the bottom of the sector as a band (hence the name analytical band analytical ultracentrifugation or AB-AUC – sometimes shorted as ABC). While the rate at which the analyte sediments is determined by its sedimentation coefficient, the band itself will also diffuse and broaden. This broadening is related to the diffusion coefficient of the analyte. If there is a mixture of two or more analytes with different sedimentation coefficients, then the experiment will result in the separation of the initial band into two or more species that reach the cell bottom at different times. This experiment, while requiring a different type of centerpiece from traditional SV-AUC, has the advantage of needing much less sample. In addition, the results can be visually interpreted, if the difference in sedimentation coefficients results in clear separation of bands. Data analysis depends on peak identification and integration to obtain relative populations of different species. This can be done using Origin, SigmaPlot or similar commercial graphing tools. This experiment was originally developed by Vinograd and co-workers at Caltech in the 1960s³⁵. Cölfen revisited this technique in the late 2010s using myoglobin and polystyrene beads as test samples^{36,37}. Khasa and co-workers used AB-AUC experiments to separate empty and full AAV particles in 2012³⁸. In this study, the authors plotted AUC scans as a function of both time and radius – a profile they termed “centrifugrams.” These centrifugrams enable the identification of peak maxima and tracking of its position with time. This allows the use of the integral form of the equation defining the sedimentation coefficient as follows:

$$s = \frac{1}{\omega^2(t-t_0)} \ln \left(\frac{r}{r_0} \right)$$

In this equation, the sedimentation coefficient is S , the angular velocity is ω , the peak maximum is seen at a radial position r at time t , where it was originally seen at a reference radial position r_0 at starting time t_0 . Thus, ABC experiments can be processed to provide sedimentation coefficient of different species if the corresponding peaks are well separated. Needless to say, with baseline separation of peaks, percentages of different populations can also be determined. Khasa showed that the results obtained for AAV empty/full ratios obtained from ABC are comparable to those obtained from SV-AUC³⁸.

Density-Matched Sedimentation-Velocity AUC

Density-Matched Sedimentation-Velocity AUC or DM-SV-AUC (sometimes more appropriately called Density-Contrast SV-AUC) is yet another variation of the SV-AUC experiment wherein the target analyte is mixed into buffer containing a percentage of heavy water (D_2O). Since heavy water has a different density (1.1050 g/mL at 20 °C) than ordinary water (0.9982 g/mL at 20 °C), it is possible to make different buffers with the same buffering agent (phosphates, TRIS, HEPES, etc.) and salts (NaCl, KCl, $CaCl_2$, etc.), but with varying densities depending on the relative fractions of water and heavy water. Performing an SV-AUC experiment with the same target analyte, but in buffers with different densities, will therefore result in different observed sedimentation behaviors. Specifically, as buffer density increases, the observed S -value of the target analyte will decrease. When the buffer density exceeds that of the target analyte, the experiment will yield floatation boundaries, as opposed to sedimentation boundaries. This phenomenon can be exploited to obtain the density (or partial specific volume) of the target analyte along with additional information. DM-SV-AUC has been demonstrated by the Demeler group for LNPs³⁹.

Sedimentation-Equilibrium AUC

During an AUC experiment, if the flux due to centrifugal acceleration is matched by the flux due to diffusion, then an equilibrium condition will be attained where there will be no net movement of analyte particles in either direction. This condition and the experiment designed to achieve it is known as sedimentation equilibrium (SE-AUC). The concentration of the analyte particle forms a gradient ranging from very low concentration at the top of the cell to maximum concentration at the bottom of the cell. The mathematical nature of the relationship between concentration and radial position is a quadratic exponential and has been independently derived by Fujita and others⁹⁻¹¹.

$$c(r) = c_0 \cdot \exp\left(\frac{M_b \cdot \omega^2}{RT} \cdot \left(\frac{r^2 - r_0^2}{2}\right)\right)$$

In this equation, the concentration $c(r)$ is a function of radius r . The reference concentration c_0 is defined at reference radius r_0 , and M_b is the buoyant mass of the analyte. The angular velocity is ω . R is the Universal Gas Constant and T is the temperature. At equilibrium, the experiment yields static scans or traces, which can be fitted to obtain precise measurements of the buoyant mass of the analyte. Since this quantity is a function of analyte state (e.g., oligomerization, aggregation, and degradation, as well as loading fraction for AAV and similar analytes) the SE experiment can be used to obtain these and other thermodynamic equilibria parameters (such as binding constants and stoichiometry).

Comparison of different AUC techniques

Sedimentation-equilibrium (SE) experiments are carried out at relatively low rotor speeds, typically over several days, and are useful for determining the molecular weight distribution of the analyte population with high accuracy^{40,41}. Analysis of SE data requires fitting experimental curves (i.e., scan data) to the SE equation shown previously. This can be done using software packages like UltraScan and SEDPHAT^{20,21,42}, but also any numerical/graphing tool such as SigmaPlot, MATLAB, etc. Sedimentation-velocity (SV) experiments, on the other hand, are carried out at relatively higher rotor speeds and for shorter durations (a few hours), and are useful for determining the sedimentation coefficient distribution of the analyte population. This distribution can be further interpreted in terms of analyte composition and can usually be converted into a mass distribution¹⁴. The analysis of SV data requires sophisticated software tools like SEDFIT and UltraScan, both of which use finite element methods to solve the Lamm equation^{14-17,19-22}. The combination of SV and SE-AUC experiments can be used to quantitatively answer several biophysical questions such as protein binding, aggregation, degradation and more⁴³⁻⁴⁶. Analytical-Band AUC or ABC experiments have been used successfully to obtain loading fractions of AAV particles by Khasa³⁸ and more recently by Bepperling⁴⁷. SV-AUC on LNPs by Guerrini and co-authors⁴⁸ has revealed significant heterogeneity in LNP formulation. This has been corroborated only by DM-SV-AUC carried out by the Demeler group³⁹, and more recently by Bepperling⁴⁹. It should be noted that the work by Guerrini used the ls-g*(s) module as implemented in SEDFIT⁵⁰. This calculation is based on the model-free time derivative analysis technique originally invented by Walter Stafford and popularized further by John Philo^{23,25,26,51,52}. However, this analysis technique does not yield high-resolution results, which are obtained by numerical solutions to the Lamm equation. The latter approach is used by Henrickson and co-authors³⁹.

Limitations of current AUC methods

1. SV-AUC experiments are size limited. Fully loaded AAV (diameter: 26 nm, mass ~ 5 MDa) capsids sediment at close to 90 S. Particles larger than this will typically sediment very fast, providing just a few scans to analyze. This is demonstrated in Fig 1C.
2. Analysis of SV-AUC data necessitates specialized software packages which implement finite element solutions to the Lamm equation^{14,15,17,19-22}. This analysis, while certainly robust, lacks visual intuitiveness and requires some training.
3. Sample requirements for SV-AUC experiments, measured in absorbance units with respect to a 10 mm path, start at a minimum of ~0.1 AU using 450 μ L of sample. This requirement is challenging for costly materials such as viral vectors. However, ABC experiments can provide fairly robust quantitation of AAV loading fractions at a fraction of the sample consumption of SV-AUC (10-20 μ L of sample).
4. SE-AUC is usually run for several days to quantitate analyte mass. Mass can usually be obtained from SV-AUC, therefore SE-AUC experiments are rarely used, especially when sample stability is of concern. However, for smaller analytes such as peptides, SV-AUC may not always achieve complete sedimentation or pelleting of the sample. In such instances, SE-AUC proves invaluable by offering robust measurements of mass distribution and percentages of aggregation populations.

New therapeutic products require improved AUC methods

A major focus area in modern biotechnology is therapeutic delivery vehicles. Liposomes have been used to encapsulate small molecule drugs, especially chemotherapeutic drugs such as doxorubicin⁵³⁻⁵⁹. Another such focus area with significant public health impact is that of mRNA vaccines encapsulated within lipid nanoparticles, or LNPs⁶⁰⁻⁶⁴. Nanoparticle-based drugs face similar quality control challenges as AAV-based gene therapy drugs, particularly regarding loading fraction and population heterogeneity. Thus, similar to SV-AUC experiments conducted on AAV samples, efforts have been made to characterize LNPs using SV-AUC. Although these do not typically achieve the same level of success as with AAV samples, DM-SV-AUC (with D₂O mixed buffer) has shown promise in LNP characterization³⁹.

Comparison of SV-AUC results obtained for AAV and LNP samples

Figure 1 illustrates the differences between the c(s) distributions of AAV and LNPs in an SV-AUC experiment.

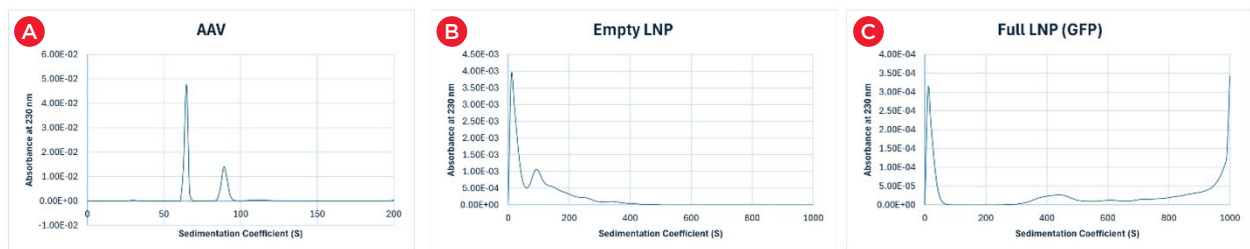


Figure 1. Comparison of (A) AAV, (B) empty LNPs, and (C) loaded LNPs in an SV-AUC experiment.

The experimental and analysis parameters and fit results for both samples are tabulated below in Table 1:

Parameter	AAV	LNP
Sample / Reference Identity	AAV9 in PBS / PBS	Empty LNP in PBS, GFP-LNP in PBS
Absorbance (230 nm)	0.18	0.67 (Empty), 0.61(Full)
Temperature (°C)	20	20
Thermal Equilibrium Delay (min)	180	20
Rotor Speed (rpm)	15,000	10,000
Total Scans	300	100
Scan Interval (sec)	180	180
Scans Analyzed	1 to 75	1 to 20
S value range	0 to 200	0 to 1000
S value points	100	100
RMSD (absolute)	0.00199	0.00375 (Empty), 0.0092 (Full)
RMSD/Signal Plateau %	1.00%	0.56% (Empty), 1.51% (Full)

Table 1. Comparison of AAV vs LNP samples in SV-AUC.

A comparison of the $c(s)$ distribution already indicates that the AAV sample is highly amenable to SV-AUC analysis and yields an excellent fit with baseline separation of empty and full capsid species. LNP samples show the presence of low-mass species, as seen in the peaks near $S = 0$, and the full LNP samples (loaded with GFP mRNA) show the presence of large aggregates as seen at the maxima of the X-axis ($S = 1000$). Taken together, this analysis suggests that the LNP samples are highly heterogeneous, likely containing a diverse population of particles, as well as potential degradation and aggregation products. Therefore, orthogonal techniques are needed to provide additional insight into the composition of LNPs.

DGE- AUC

Introduction to DGE-AUC

SV-AUC can be complemented by a technique called density gradient equilibrium analytical ultracentrifugation (DGE-AUC). The origins of this technique lie in the famous Meselson/Stahl experiment of 1958, which was mentioned previously⁵. The operating principle is as follows: analyte particles are mixed with a gradient forming material (GFM) and centrifuged at high speed. At equilibrium, the GFM forms a density gradient from the top to the bottom of the AUC sample cell following the same quadratic exponential curve shape that is obtained in a sedimentation equilibrium experiment⁶. This is the first of two transport processes which are occurring simultaneously in the AUC cell. The first relates to the GFM while the second relates to the movement of the actual analyte particle, which may be a protein, a nucleic acid, a virus, a nanoparticle, etc. The second transport process also attains its own equilibrium wherein different analyte particles in solution will migrate to a radial position where the local density of the GFM is equal to the buoyant density of the analyte itself. Thus, DGE-AUC experiments separate analytes on the basis of their buoyant densities. In a mixture of AAV capsids containing fully loaded and empty capsids we would expect the fully loaded capsids (which are high-density particles) to stabilize at a radial position further down the sample tube as compared to empty capsids (which are low-density particles). A similar effect is seen for drug-carrying nanoparticles where the empty nanoparticle has a different density from the drug-loaded nanoparticle.

In recent years, DGE-AUC has seen a resurgence in interest, primarily driven by the need to characterize larger analytes^{47,65-67}. Beckman Coulter Life Sciences provides online resources for getting started with DGE-AUC⁶⁸, including this article in EBJ which covers some aspects of DGE-AUC method optimization⁶⁶.

Simulating an equilibrium density gradient

As discussed previously, the shape of a density gradient at equilibrium is mathematically defined by a quadratic exponential equation. Thus, it is possible to simulate the equilibrium shape of a density gradient by considering the starting concentration of the GFM, the temperature, the rotor speed, and the mathematical relationship between the density and the concentration of the GFM. The results of simulating density gradients for a solution of cesium chloride (CsCl) at 20° C is shown in Figure 2. The shape of a density gradient is concave upwards. The density gradient can be considered to pivot around the radial position which corresponds to the starting density of GFM when the rotor is stationary. This radial position is known as the pivot point or the isodensity point. At higher rotor speeds, the gradient shape becomes progressively steeper but always passes through the pivot point.

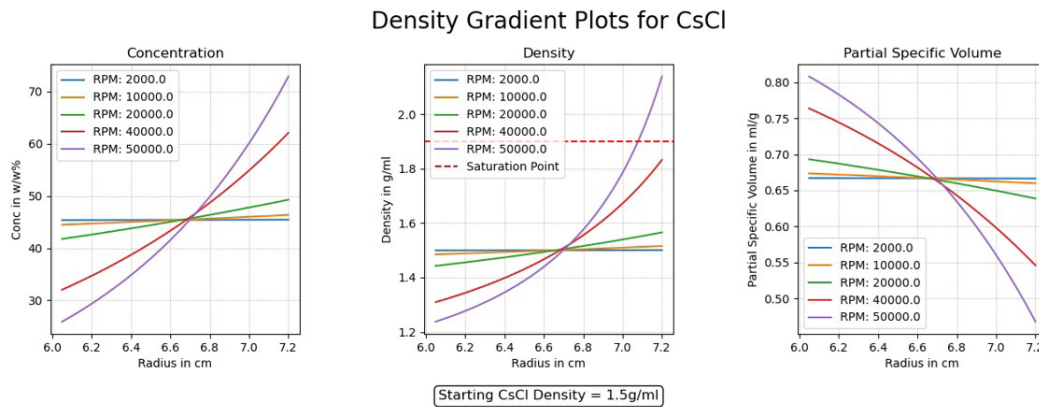


Figure 2. Simulating density gradients for CsCl at different rotor speeds.

Why simulate density gradient curves?

1. Experimental Safety: It can be seen that at high rotor speeds the maximum density attained by the gradient forming material can exceed its saturation density, leading to precipitation and imbalancing. This should be avoided at all costs because it can cause damage to the rotor and the centrifuge. Therefore, it is advisable whenever possible to simulate the shape of the density gradient before performing an actual experiment.
2. Predicting the location of analytes: In addition, such a simulation also allows us to predict the equilibrium radial positions of different analyte particles if we know their buoyant densities based upon theoretical models or orthogonal measurements. This is shown in Figure 3.

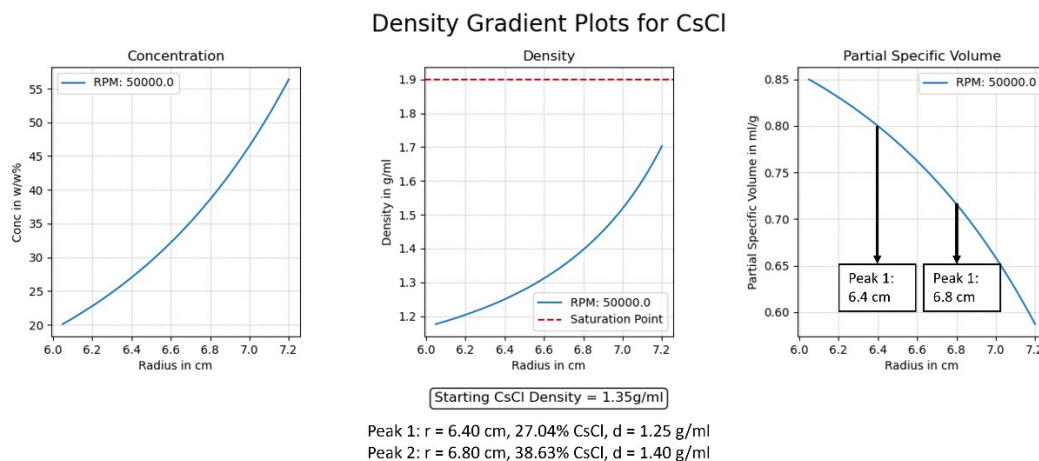


Figure 3. Using DGE simulations to predict the positions of analytes of known densities.

Summary and Discussion

There are several orthogonal AUC techniques which are used to characterize complex drug carrier systems (vectors) such as virus particles, nanoparticles and more^{32,47,49,65-67,69}. This table shows a comparison of these different techniques:

Technique	SV-AUC	SE-AUC	DM-SV-AUC	ABC-AUC	DGE-AUC
Separation principle	Sedimentation Coefficient	Mass	Sedimentation Coefficient (and density)	Sedimentation Coefficient	Buoyant density
Physical Principle	Sedimentation or floatation of sample	Equilibrium gradient of sample	Sedimentation or floatation of sample in mixed density buffer	Sedimentation or floatation of sample band	Band formation by analyte in an equilibrium gradient of salt/sucrose/ other GFM
Duration	Few hours	Few days	Few hours	Few hours	1-2 days
Number of experiments / samples required for analysis (post optimization)	1	1	Several samples with different buffer densities	1	1
Buffer conditions	Native (PBS, etc.)	Native (PBS, etc.)	Native (PBS, etc.) but with D2O/H2O mix.	Native (PBS, etc.)	Requires gradient forming material like CsCl, sucrose, etc.
Sample requirements per experiment	- 400 μ L at Abs230 = 0.5	- 100 μ L at Abs230 = 0.5	- 400 μ L at Abs230 = 0.5	- 15 μ L at Abs230 = 0.5	- 20 μ L at Abs230 = 0.5
What AUC cells are used?	2-sector standard/ flow-through SV cells	6-sector SE cells	2-sector standard/ flow-through SV cells	2-sector band forming cells	2-sector standard/ flow-through SV cells
Analysis Principle	Solve Lamm Equation	Solve SE equation	Solve Lamm Equation	Solve Svedberg / Lamm Equation	Visualize and integrate
Software needed	SEDFIT/UltraScan	SEDPHAT/ UltraScan	SEDFIT/UltraScan	SEDFIT/ UltraScan (for Lamm Equation) or SigmaPlot/ GraphPad/Origin (for Svedberg Equation)	Excel/SigmaPlot/ GraphPad/Origin
Result/Output	Population distribution of sedimentation coefficient	Population distribution of mass	Population distribution of sedimentation coefficient	Population distribution of sedimentation coefficient	Population distribution of density
Size limitation?	yes	no	yes	yes	no

In summary

1. SV-AUC separates analytes based on sedimentation coefficient and SE-AUC on the basis of mass differences. DM-SV-AUC is a variant of SV-AUC which uses mixed H₂O-D₂O buffer. ABC is yet another variant of SV-AUC in which the analyte is present as a thin band layered on top of the buffer, as opposed to being homogeneously distributed throughout the buffer volume.
2. These AUC techniques are used to characterize the size, mass and shape of analyte particles. These fundamental physical parameters can then be used to extract higher order information such as binding constants, stoichiometry, oligomerization, heterogeneity, aggregation and degradation states.
3. DGE-AUC is an orthogonal method that separates analyte particles on the basis of their buoyant densities. This technique, based on the classic Meselson-Stahl experiment in 1958, is enjoying a resurgence because it provides a useful complement to the more established AUC techniques.
4. DGE-AUC has the following advantages:
 - a. No effective size limitation.
 - b. DGE-AUC requires very little sample.
 - c. DGE-AUC data can be visually interpreted and analyzed with commonly used graphing software like Origin, GraphPad Prism, SigmaPlot, IgorPro, or even Excel.
5. DGE-AUC gradient curves can be simulated for different gradient forming materials (GFMs) at different temperatures and rotor speeds, which is useful for predicting the equilibrium position of various analytes.

In subsequent installments of Demystifying DGE, we will cover experiment setup and optimization, interpretation and analysis of results.

Disclaimer

1. Several third-party software vendors supply programs for the analyses of the raw data generated by the Beckman Coulter Inc. (“Beckman”) Analytical Ultracentrifuge. Third-party analysis software has not been validated by Beckman for use with the Beckman Analytical Ultracentrifuge. Training conducted by Beckman on the third-party software, does not imply a recommendation for use or the suitability of the third-party software use by the customer. Beckman does not endorse any third-party analyses software. Beckman warranty and/or performance guarantee that may be applicable or are provided by Beckman for Beckman Analytical Ultracentrifuge do not apply to any third-party software.
2. Copyright, License and Terms of Use Disclaimers are documented for the below software on their respective pages. For example:
 - a. SEDDFIT: <https://sedfitedphat.nibib.nih.gov/software/default.aspx>
 - b. OriginLab: <https://www.originlab.com/index.aspx?go=Company/TermsOfUse>
 - c. Ultrascan: <http://ultrascan.aucsolutions.com/license.php>
 - d. Microsoft: <https://www.microsoft.com/en-us/useterms/>
 - e. Gussi: <https://www.utsouthwestern.edu/labs/mbr/software/>
 - f. Python: <https://www.python.org/>
 - g. Matplotlib: <https://matplotlib.org/>

- h. NumPy: <https://numpy.org/>
 - i. SciPy: <https://scipy.org/>
 - j. MATLAB: <https://www.mathworks.com/products/matlab.html>
3. Beckman Coulter makes no warranties of any kind whatsoever express or implied, with respect to this protocol, including but not limited to warranties of fitness for a particular purpose or merchantability or that the protocol is non-infringing. All warranties are expressly disclaimed. Your use of the method is solely at your own risk, without recourse to Beckman Coulter. Not intended or validated for use in the diagnosis of disease or other conditions. This protocol is for demonstration only and is not validated by Beckman Coulter.
 4. Regulatory / Trademark Statements:
 - a. All products and services identified, unless noted as for in-vitro diagnostic (IVD) use, are for research use and not intended or validated for use in the diagnosis of disease or other conditions.
 - b. ©2024 Beckman Coulter, Inc. Beckman Coulter, the stylized logo, and the Beckman Coulter product and service marks mentioned herein are trademarks or registered trademarks of Beckman Coulter, Inc. in the United States and other countries.
 - c. All other trademarks are the property of their respective owners.

References

1. Nobel Prize Physics 1926 Summary, <<https://www.nobelprize.org/prizes/physics/1926/summary/>> (1926).
2. Kyle, R. A. & Shampo, M. A. Theodor Svedberg and the ultracentrifuge. Mayo Clin Proc 72, 830 <https://doi.org/10.4065/72.9.830>
3. Pedersen, K. O. The development of Svedberg's ultracentrifuge. Biophys Chem 5, 3-18 [https://doi.org/10.1016/0301-4622\(76\)80022-1](https://doi.org/10.1016/0301-4622(76)80022-1)
4. Creeth, J. M. From oil-turbine to Model E: early days in retrospect. Macromol Biosci 10, 693-695 (2010). <https://doi.org/10.1002/mabi.200900370>
5. Meselson, M. & Stahl, F. W. THE REPLICATION OF DNA IN ESCHERICHIA COLI. Proc Natl Acad Sci U S A 44, 671-682 <https://doi.org/10.1073/pnas.44.7.671>
6. Cole, J. L., Lary, J. W., P Moody, T. & Laue, T. M. Analytical ultracentrifugation: sedimentation velocity and sedimentation equilibrium. Methods Cell Biol 84, 143-179 (2008). [https://doi.org/10.1016/S0091-679X\(07\)84006-4](https://doi.org/10.1016/S0091-679X(07)84006-4)
7. Zhao, H., Brautigam, C. A., Ghirlando, R. & Schuck, P. Overview of current methods in sedimentation velocity and sedimentation equilibrium analytical ultracentrifugation. Curr Protoc Protein Sci 20, 1-12 <https://doi.org/10.1002/0471140864.ps2012s71>
8. Lamm, O. Die Differentialgleichung der Ultrazentrifugierung. Arkiv för Matematik, Astronomi och Fysik (1929).
9. Fujita, H. Foundations of ultracentrifugal analysis. (John Wiley & Sons, 1975).
10. Williams, J. W., Van Holde, K. E., Baldwin, R. L. & Fujita, H. Chemical Reviews. Chemical Reviews 58, 715-744 (1958). <https://doi.org/10.1021/cr50022a005>

11. Tanford, C. & Huggins, M. L. J. Electrochem. Soc. Journal of The Electrochemical Society 109, 98C (1962).
12. Claverie, J. M., Dreux, H. & Cohen, R. Sedimentation of generalized systems of interacting particles. I. Solution of systems of complete Lamm equations. Biopolymers 14, 1685-1700 (1975).
<https://doi.org/10.1002/bip.1975.360140811>
13. Holladay, L. A. An approximate solution to the Lamm equation. Biophys Chem 10, 187-190 (1979).
[https://doi.org/10.1016/0301-4622\(79\)85039-5](https://doi.org/10.1016/0301-4622(79)85039-5)
14. Schuck, P. Size-distribution analysis of macromolecules by sedimentation velocity ultracentrifugation and lamm equation modeling. Biophys J 78, 1606-1619 (2000).
[https://doi.org/10.1016/S0006-3495\(00\)76713-0](https://doi.org/10.1016/S0006-3495(00)76713-0)
15. Schuck, P. Sedimentation analysis of noninteracting and self-associating solutes using numerical solutions to the Lamm equation. Biophys J 75, 1503-1512 (1998). [https://doi.org/10.1016/S0006-3495\(98\)74069-X](https://doi.org/10.1016/S0006-3495(98)74069-X)
16. Cao, W. & Demeler, B. Modeling analytical ultracentrifugation experiments with an adaptive space-time finite element solution of the Lamm equation. Biophys J 89, 1589-1602 (2005).
<https://doi.org/10.1529/biophysj.105.061135>
17. Demeler, B. & Saber, H. Determination of molecular parameters by fitting sedimentation data to finite-element solutions of the Lamm equation. Biophys J 74, 444-454 (1998).
[https://doi.org/10.1016/S0006-3495\(98\)77802-6](https://doi.org/10.1016/S0006-3495(98)77802-6)
18. Beckman Analytical Ultracentrifuges, <<https://www.beckman.com/centrifuges/analytical-ultracentrifuges/optima-auc>> (2023).
19. Schuck, P. SEDFIT-SEDPHAT, <<https://sedfitsedphat.github.io/>> (
20. Demeler, B. UltraScan version XXX. A Comprehensive Data Analysis Software Package for Analytical Ultracentrifugation Experiments, <<http://www.ultrascan.aucsolutions.com>>
21. Demeler, B. in Modern Analytical Ultracentrifugation: Techniques and Methods (eds D. J. Scott, S. E. Harding, & A. J. Rowe) 210-229 (Royal Society of Chemistry (UK), 2005).
22. Demeler, B. in Bioinformatics Basics: Applications in Biological Science and Medicine (eds H. Rashidi & L. Buehler) 226-255 (CRC Press LLC, 2005).
23. Stafford, W. in Biophysical Journal Vol. Biophysical Journal (1998).
24. Stafford, W. Analytical ultracentrifugation: sedimentation velocity analysis. Curr Protoc Protein Sci 20 (2003). <https://doi.org/10.1002/0471140864.ps2007s31>
25. Stafford, W. F., 3rd. Boundary analysis in sedimentation transport experiments: a procedure for obtaining sedimentation coefficient distributions using the time derivative of the concentration profile. Anal Biochem 203, 295-301 (1992). [https://doi.org/10.1016/0003-2697\(92\)90316-y](https://doi.org/10.1016/0003-2697(92)90316-y)
26. Philo, J. S. An improved function for fitting sedimentation velocity data for low-molecular-weight solutes. Biophys J 72, 435-444 (1997). [https://doi.org/10.1016/s0006-3495\(97\)78684-3](https://doi.org/10.1016/s0006-3495(97)78684-3)
27. Wang, C. et al. Developing an Anion Exchange Chromatography Assay for Determining Empty and Full Capsid Contents in AAV6.2. Mol Ther Methods Clin Dev 15, 257-263 (2019).
<https://doi.org/10.1016/j.omtm.2019.09.006>
28. Grimm, D. & Büning, H. Small But Increasingly Mighty: Latest Advances in AAV Vector Research, Design, and Evolution. Hum Gene Ther 28, 1075-1086 (2017). <https://doi.org/10.1089/hum.2017.172>

29. Naso, M. F., Tomkowicz, B., Perry, W. L., 3rd & Strohl, W. R. Adeno-Associated Virus (AAV) as a Vector for Gene Therapy. *BioDrugs* 31, 317-334 (2017). <https://doi.org/10.1007/s40259-017-0234-5>
30. Santiago-Ortiz, J. L. & Schaffer, D. V. Adeno-associated virus (AAV) vectors in cancer gene therapy. *J Control Release* 240, 287-301 (2016). <https://doi.org/10.1016/j.jconrel.2016.01.001>
31. Burnham, B. et al. Analytical Ultracentrifugation as an Approach to Characterize Recombinant Adeno-Associated Viral Vectors. *Hum Gene Ther Methods* 26, 228-242 (2015). <https://doi.org/10.1089/hgtb.2015.048>
32. Maruno, T., Usami, K., Ishii, K., Torisu, T. & Uchiyama, S. Comprehensive Size Distribution and Composition Analysis of Adeno-Associated Virus Vector by Multiwavelength Sedimentation Velocity Analytical Ultracentrifugation. *J Pharm Sci* 110, 3375-3384 (2021). <https://doi.org/10.1016/j.xphs.2021.06.031>
33. Richter, K. et al. Purity and DNA content of AAV capsids assessed by analytical ultracentrifugation and orthogonal biophysical techniques. *Eur J Pharm Biopharm* 189, 68-83 (2023). <https://doi.org/10.1016/j.ejpb.2023.05.011>
34. Saleun, S. et al. Analytical ultracentrifugation sedimentation velocity for the characterization of recombinant adeno-associated virus vectors sub-populations. *Eur Biophys J* 52, 367-377 (2023). <https://doi.org/10.1007/s00249-023-01650-3>
35. Vinograd, J., Bruner, R., Kent, R. & Weigle, J. Band-centrifugation of macromolecules and viruses in self-generating density gradients. *Proc Natl Acad Sci U S A* 49, 902-910 (1963). <https://doi.org/10.1073/pnas.49.6.902>
36. Schneider, C. M. & Colfen, H. Analytical band centrifugation revisited. *Eur Biophys J* 47, 799-807 (2018). <https://doi.org/10.1007/s00249-018-1315-1>
37. Schneider, C. M., Haffke, D. & Colfen, H. Band Sedimentation Experiment in Analytical Ultracentrifugation Revisited. *Anal Chem* 90, 10659-10663 (2018). <https://doi.org/10.1021/acs.analchem.8b02768>
38. Khasa, H., Kilby, G., Chen, X. & Wang, C. Analytical band centrifugation for the separation and quantification of empty and full AAV particles. *Mol Ther Methods Clin Dev* 21, 585-591 (2021). <https://doi.org/10.1016/j.omtm.2021.04.008>
39. Henrickson, A. et al. Density Matching Multi-wavelength Analytical Ultracentrifugation to Measure Drug Loading of Lipid Nanoparticle Formulations. *ACS Nano* 15, 5068-5076 (2021). <https://doi.org/10.1021/acsnano.0c10069>
40. Taylor, I. A., Eccleston, J. F. & Rittinger, K. Sedimentation equilibrium studies. *Methods Mol Biol* 261, 119-136 (2004). <https://doi.org/10.1385/1-59259-762-9:119>
41. Teller, D. C. Characterization of proteins by sedimentation equilibrium in the analytical ultracentrifuge. *Methods Enzymol* 27, 346-441 (1973). [https://doi.org/10.1016/s0076-6879\(73\)27017-9](https://doi.org/10.1016/s0076-6879(73)27017-9)
42. Vistica, J. et al. Sedimentation equilibrium analysis of protein interactions with global implicit mass conservation constraints and systematic noise decomposition. *Anal Biochem* 326, 234-256 (2004). <https://doi.org/10.1016/j.ab.2003.12.014>
43. Berkowitz, S. A. Role of analytical ultracentrifugation in assessing the aggregation of protein biopharmaceuticals. *AAPS J* 8, E590-E605 (2006). <https://doi.org/10.1208/aapsj080368>
44. Cole, J. L. & Hansen, J. C. Analytical ultracentrifugation as a contemporary biomolecular research tool. *J Biomol Tech* 10, 163-176 (1999).

45. Laue, T. M. & Stafford, W. F., 3rd. Modern applications of analytical ultracentrifugation. *Annu Rev Biophys Biomol Struct* 28, 75-100 (1999). <https://doi.org/10.1146/annurev.biophys.28.1.75>
46. Uchiyama, S., Noda, M. & Krayukhina, E. Sedimentation velocity analytical ultracentrifugation for characterization of therapeutic antibodies. *Biophys Rev* 10, 259-269 (2018). <https://doi.org/10.1007/s12551-017-0374-3>
47. Bepperling, A. & Best, J. Comparison of three AUC techniques for the determination of the loading status and capsid titer of AAVs. *Eur Biophys J* 52, 401-413 (2023). <https://doi.org/10.1007/s00249-023-01661-0>
48. Guerrini, G., Mehn, D., Scaccabarozzi, D., Gioria, S. & Calzolari, L. Analytical Ultracentrifugation to Assess the Quality of LNP-mRNA Therapeutics. *International Journal of Molecular Sciences* 25 (2024).
49. Bepperling, A. & Richter, G. Determination of mRNA copy number in degradable lipid nanoparticles via density contrast analytical ultracentrifugation. *Eur Biophys J* 52, 393-400 (2023). <https://doi.org/10.1007/s00249-023-01663-y>
50. Schuck, P. & Rossmannith, P. Determination of the sedimentation coefficient distribution by least-squares boundary modeling. *Biopolymers* 54, 328-341 (2000). [https://doi.org/10.1002/1097-0282\(20001015\)54:5<328::AID-BIP40>3.0.CO;2-P](https://doi.org/10.1002/1097-0282(20001015)54:5<328::AID-BIP40>3.0.CO;2-P)
51. Philo, J. S. A method for directly fitting the time derivative of sedimentation velocity data and an alternative algorithm for calculating sedimentation coefficient distribution functions. *Anal Biochem* 279, 151-163 (2000). <https://doi.org/10.1006/abio.2000.4480>
52. Stafford, W. F., 3rd. Boundary analysis in sedimentation velocity experiments. *Methods Enzymol* 240, 478-501 (1994). [https://doi.org/10.1016/s0076-6879\(94\)40061-x](https://doi.org/10.1016/s0076-6879(94)40061-x)
53. Abraham, S. A. et al. The liposomal formulation of doxorubicin. *Methods Enzymol* 391, 71-97 (2005). [https://doi.org/10.1016/S0076-6879\(05\)91004-5](https://doi.org/10.1016/S0076-6879(05)91004-5)
54. Bulbake, U., Doppalapudi, S., Kommineni, N. & Khan, W. Liposomal Formulations in Clinical Use: An Updated Review. *Pharmaceutics* 9, 12 (2017). <https://doi.org/10.3390/pharmaceutics9020012>
55. Tardi, P. G., Boman, N. L. & Cullis, P. R. Liposomal doxorubicin. *J Drug Target* 4, 129-140 (1996). <https://doi.org/10.3109/10611869609015970>
56. Guimarães, D., Cavaco-Paulo, A. & Nogueira, E. Design of liposomes as drug delivery system for therapeutic applications. *Int J Pharm* 601, 120571 (2021). <https://doi.org/10.1016/j.ijpharm.2021.120571>
57. Liu, P., Chen, G. & Zhang, J. A Review of Liposomes as a Drug Delivery System: Current Status of Approved Products, Regulatory Environments, and Future Perspectives. *Molecules* 27, 1372 (2022). <https://doi.org/10.3390/molecules27041372>
58. Fulton, M. D. & Najahi-Missaoui, W. Liposomes in Cancer Therapy: How Did We Start and Where Are We Now. *Int J Mol Sci* 24, 6615 (2023). <https://doi.org/10.3390/ijms24076615>
59. Sheoran, S., Arora, S., Samsonraj, R., Govindaiah, P. & Vuree, S. Lipid-based nanoparticles for treatment of cancer. *Heliyon* 8, e09403 (2022). <https://doi.org/10.1016/j.heliyon.2022.e09403>
60. Chaudhary, N., Weissman, D. & Whitehead, K. A. mRNA vaccines for infectious diseases: principles, delivery and clinical translation. *Nat Rev Drug Discov* 20, 817-838 (2021). <https://doi.org/10.1038/s41573-021-00283-5>

61. Hou, X., Zaks, T., Langer, R. & Dong, Y. Lipid nanoparticles for mRNA delivery. *Nat Rev Mater* 6, 1078-1094 (2021). <https://doi.org/10.1038/s41578-021-00358-0>
62. Reichmuth, A. M., Oberli, M. A., Jaklenec, A., Langer, R. & Blankschtein, D. mRNA vaccine delivery using lipid nanoparticles. *Ther Deliv* 7, 319-334 (2016). <https://doi.org/10.4155/tde-2016-0006>
63. Schoenmaker, L. et al. mRNA-lipid nanoparticle COVID-19 vaccines: Structure and stability. *Int J Pharm* 601, 120586 (2021). <https://doi.org/10.1016/j.ijpharm.2021.120586>
64. Samaridou, E., Heyes, J. & Lutwyche, P. Lipid nanoparticles for nucleic acid delivery: Current perspectives. *Adv Drug Deliv Rev* 154-155, 37-63 (2020). <https://doi.org/10.1016/j.addr.2020.06.002>
65. Hirohata, K. et al. Applications and Limitations of Equilibrium Density Gradient Analytical Ultracentrifugation for the Quantitative Characterization of Adeno-Associated Virus Vectors. *Anal Chem* 96, 642-651 (2024). <https://doi.org/10.1021/acs.analchem.3c01955>
66. Sternisha, S. M., Wilson, A. D., Bouda, E., Bhattacharya, A. & VerHeul, R. Optimizing high-throughput viral vector characterization with density gradient equilibrium analytical ultracentrifugation. *Eur Biophys J* 52, 387-392 (2023). <https://doi.org/10.1007/s00249-023-01654-z>
67. Yang, X., Agarwala, S., Ravindran, S. & Vellekamp, G. Determination of particle heterogeneity and stability of recombinant adenovirus by analytical ultracentrifugation in CsCl gradients. *J Pharm Sci* 97, 746-763 (2008). <https://doi.org/10.1002/jps.21008>
68. Density Gradient Equilibrium (DGE) AUC Resources Center, <<https://www.beckman.com/resources/technologies/analytical-ultracentrifugation/dge-auc-simply-auc/learning-center>>
69. Maruno, T., Ishii, K., Torisu, T. & Uchiyama, S. Size Distribution Analysis of the Adeno-Associated Virus Vector by the c(s) Analysis of Band Sedimentation Analytical Ultracentrifugation with Multiwavelength Detection. *J Pharm Sci* 112, 937-946 (2023). <https://doi.org/10.1016/j.xphs.2022.10.023>

©2024 Beckman Coulter, Inc. All rights reserved. Beckman Coulter, the Stylized Logo, and Beckman Coulter product and service marks mentioned herein are trademarks or registered trademarks of Beckman Coulter, Inc. in the United States and other countries. All other trademarks are the property of their respective owners. For research use only. Not for use in diagnostic procedures.

Several third-party software vendors supply programs for the analyses of the raw data generated by the Beckman Coulter Inc. ("Beckman") Analytical Ultracentrifuge. Third-party analysis software has not been validated by Beckman for use with the Beckman Analytical Ultracentrifuge. Training conducted by Beckman on the third-party software, does not imply a recommendation for use or the suitability of the third-party software use by the customer. Beckman does not endorse any third-party analyses software. Beckman warranty and/or performance guarantee that may be applicable or are provided by Beckman for Beckman Analytical Ultracentrifuge do not apply to any third-party software. Copyright, License and Terms of Use Disclaimers are documented for the below software on their respective pages.

For Beckman Coulter's worldwide office locations and phone numbers, please visit Contact Us at [beckman.com](https://www.beckman.com)
2024-GBL-EN-105867-v1

